



# Groundwater Geochemistry and its Impacts on Groundwater Arsenic Enrichment, Variation, and Health Risks in Yongning County, Yinchuan Plain of Northwest China

Miaojun Wei<sup>1,2</sup> · Jianhua Wu<sup>1,2</sup> · Wenqu Li<sup>1,2</sup> · Qixiao Zhang<sup>1,2</sup> · Fengmei Su<sup>1,2</sup> · Yuanhang Wang<sup>1,2</sup>

Received: 24 January 2021 / Revised: 7 March 2021 / Accepted: 13 March 2021 / Published online: 1 April 2021  
© The Author(s), under exclusive licence to Springer Nature B.V. 2021

## Abstract

High arsenic (As) groundwater is a serious environmental problem in Yinchuan Plain, northwest China. Though some measures have been taken to alleviate it, the detection rate of high As in groundwater is still high. In order to understand the occurrence and enrichment of As in groundwater and the hydrochemical evolution, correlation analysis and interpolation approach were used to interpret the spatiotemporal variation of major ions and contaminants in phreatic groundwater at 30 sampling sites during the dry season (March) and wet season (July). Some suggestions on the treatment of groundwater As pollution in the study area were put forward. The results reveal that the predominant hydrochemical type of groundwater in the study area is  $\text{SO}_4\text{-Cl-Ca-Mg}$ , followed by  $\text{HCO}_3\text{-Ca-Mg}$  type, and rock weathering is the main process regulating the hydrochemical characteristics. The content of groundwater As is low in the dry season but high in the wet season. However, the difference of As concentration between the dry and wet seasons is relatively small in the areas where surface water percolation is intense. The concentrations of  $\text{HCO}_3^-$ ,  $\text{NH}_4^+$ ,  $\text{PO}_4^{3-}$ , and Mn have a significantly positive correlation with the As enrichment in the dry season, while  $\text{HCO}_3^-$ , Fe, and Mn have a strongly negative correlation with As in the wet season. The content of As in surface water influences greatly to the As enrichment in groundwater. In the dry season, high arsenic is enriched in areas close to surface water, while in the wet season, the infiltration of irrigation water makes arsenic expand to the western agricultural irrigation area. The mean lung cancer risk caused by As is higher than the maximum acceptable level in the study area. As such, necessary actions such as adopting nanocomposites as As removal material are to be carried out.

**Keywords** Arsenic pollution · Groundwater quality · Kriging interpolation · Correlation analysis · Yellow River · Health risk

## Introduction

Globalization, urbanization, and industrialization has increased the demand on resources, such as water, mineral, and new clean energy, which has attracted great attention from both policy makers and researchers (Li et al. 2012; Delgado et al. 2010). Groundwater is an important part of water resources. Many countries in the world use groundwater for

municipal, industrial, and agricultural purposes. In some areas where surface water is scarce, groundwater is even used as the only source of drinking water (Wang et al. 2020). Therefore, the quality of the groundwater is fundamental to ensure the safety of groundwater supply.

Arsenic (As) is a non-metallic element and it exists in soil, rock, surface water and groundwater in both organic and inorganic forms (Bibi et al. 2015). As can be very toxic, especially in the form of  $\text{As}^{3+}$ . When the As content in the groundwater exceeds 10  $\mu\text{g/L}$ , the groundwater is considered contaminated and its consumption will pose a threat to human health (He et al. 2020a). High levels of As exposure (> 50  $\mu\text{g/L}$ ) can cause bladder, various cancers such as lung cancer, liver cancer, kidney cancer, and skin cancer (Sultana et al. 2014). Studies have already found that exposure to As by dermal contact can adversely affect a woman's pregnancy (Chakraborti et al. 2016). Therefore, the World

✉ Jianhua Wu  
wjh2005xy@126.com; wujianhua@chd.edu.cn

<sup>1</sup> School of Water and Environment, Chang'an University, No. 126 Yanta Road, Xi'an 710054, Shaanxi, China

<sup>2</sup> Key Laboratory of Subsurface Hydrology and Ecological Effects in Arid Region of the Ministry of Education, Chang'an University, No. 126 Yanta Road, Xi'an 710054, Shaanxi, China

Health Organization (WHO) set the permissible limit of As in drinking water at 10  $\mu\text{g/L}$  (WHO 2011) to ensure the safety of drinking water.

Most of the As in surface water exists as  $\text{As}^{5+}$ , while  $\text{As}^{3+}$  is more common in the relatively anoxic underground environment.  $\text{As}^{3+}$  is more active and more likely to react with sulfate and alcohol proteins than  $\text{As}^{5+}$ , so groundwater As pollution is considered a more serious problem than surface water As pollution (Basu et al. 2001). Therefore, a number of studies have been carried out on the health problems caused by groundwater As pollution (Jang et al. 2008; Baig et al. 2011; Sultana et al. 2014). Estimated daily intake (EDI), target hazard quotient (THQ), and hazard quotient (HQ) values are commonly used to assess the health risks caused by pollution (Baig et al. 2011). Some studies have revealed a significant correlation between As and  $\text{PO}_4^{3-}$ ,  $\text{F}^-$ , Fe, and pH in groundwater, which is governed by natural processes such as adsorption/desorption and oxidation/reduction (Smedley et al. 2005). However, anthropogenic activities can also increase the content of As in groundwater, such as excessive use of fertilizers and pesticides, unlicensed and untested sewage systems, and improper disposal of sludge and solid waste (Radford et al. 2018). Several studies have shown that groundwater level fluctuation can significantly affect the occurrence forms of As. Therefore, the change of phreatic groundwater flow system caused by artificial pumping can cause a noticeable impact on groundwater As pollution (McBean 2012). Biswas et al. (2013) considered these seasonal effects and determined the As levels in irrigated water, soil, and grain and analyzed the relationship between these factors. In recent years, multivariate statistical techniques such as principal component analysis (PCA) and factor analysis (CA) were widely used to identify the chemical changes in groundwater and the factors affecting the content of As in different hydrochemical environments (Islam et al. 2017). At present, the widely used arsenic removal technologies include membranes, coagulation, ion exchange, disposable iron media, softening, etc. (Basu et al. 2013). Nano-adsorbents such as nanoparticles of titanium dioxide, zinc oxide, CuO (copper oxide), and mixed metal oxides have been used to remove arsenic from groundwater (Arora. 2021). Maity et al. (2019) compared the adsorption performance of new natural magnetic rock materials (NMM) and synthetic magnetic materials (SMM) in situ and ex situ groundwater arsenic removal. Their results show that the NMM rock materials are suitable for the removal of arsenic in groundwater. All these existing researches are important and have accelerated the progress of groundwater As research.

Groundwater As pollution in China was first identified in the 1960s. Surveys have revealed the presence of groundwater As in 20 provinces of China, and most of the high As groundwater is found in arid and semi-arid areas and river deltas. It is reported that about 36,000 residents

are threatened by high-As groundwater in China (Guo et al. 2014). Yinchuan Plain, Hetao Plain, Huhhot Plain, Datong Plain, and Yuncheng Basin have been identified as arsenicosis endemic regions (Wen et al. 2013). As poisoning in the Yinchuan Plain was first discovered in 1995 (Guo et al. 2014). The high-As groundwater in Yinchuan Plain is mainly discovered in the north of the plain and distributed along the two ancient Yellow River channels in a strip with a length of about 100 km (Wen et al. 2013). Li et al. (2018) used Monte Carlo method to quantify the uncertainty of risk assessment of potential As pollution in Jiangnan plain. The results showed that the risks caused by As had significant seasonal differences, with higher values in the rainy season and lower values in the dry season (Li et al. 2018). These groundwater As research focused mainly on the hydrochemical evolution and the health risk assessment of groundwater As (Li et al. 2018; Bian et al. 2015; Chen et al. 2017).

Though much attention has been paid to groundwater As research in recent year in Yinchuan Plain, the significant seasonal effect and spatial variation of groundwater As pollution in the Yinchuan plain have not been fully understood. Therefore, in this study, multivariate statistical techniques were used to identify the hydrogeochemical processes of groundwater As in Yongning County of the Yinchuan Plain, and the spatiotemporal variation of As was determined by Kriging interpolation method. The results will help many researchers to gain further understanding into the distribution and migration of arsenic contamination in the study area. It will also be the theoretical basis for the local decision makers to take action for the subsequent prevention and control of arsenic pollution.

## Study Area

### Location, Climate, and Hydrology

The study area is located in Yongning county, central Yinchuan Plain of Ningxia Autonomous Region, stretching within longitude 106°00'36"-106°31'20"E and latitude 38°20'51"-38°38'25"N. The entire Yinchuan Plain can be divided into piedmont alluvial inclined plain, alluvial plain, and alluvial and lacustrine plain from west to east. It belongs to the arid continental climate, with a rapid warming spring, a short summer and autumn, and a long winter. The annual temperature in this area varies greatly, with the annually average minimum temperature of  $-20.8\text{ }^\circ\text{C}$  in winter, and the annually average maximum temperature of  $35.9\text{ }^\circ\text{C}$  in summer. The rainfall in this area is limited but the sunshine is abundant (Wu et al. 2015). The average annual precipitation is 182.6 mm, and the evaporation in the study area is approximately ten times of the rainfall. The rainfall is mainly concentrated from July to September, and the rainfall

in these three months accounts for about 70% of the total rainfall in a year.

Yinchuan basin is a fault basin formed in the Cenozoic age with an overall stretching trend of NNE. The thickness of the Cenozoic formation can be 7000 m, and the maximum thickness of the Quaternary deposits is over 2000 m (Qian et al. 2012, 2013). The study area has an agricultural history of over 2000 year by diverting water from the Yellow River. The first agricultural irrigation period starts in late April every year and stops in middle September. The second irrigation period ranges from the middle November to late December. The percolation of canal water and infiltration of irrigation water can promote a great impact on groundwater. The dynamics of phreatic groundwater vary correspondingly to the irrigation period. March represents the dry season, while July represents the wet season in the study area (Fig. 1).

### Hydrogeology

According to the groundwater occurrence conditions and lithologic characteristics in the Yinchuan Plain, the main focus of the present study is the loose rock pore water. The whole plain can be divided into single phreatic water zone and multi-layer structure groundwater zone (Fig. 2) according to the geology, geomorphology, and hydrogeological conditions (Qian et al. 2013), while the present study area is mainly situated in the multi-layer structure groundwater zone.

The single phreatic groundwater is mainly distributed along the foot of the mountains in the west of the plain (mainly the piedmont alluvial inclined plain), while the multi-layer structure groundwater is found in the alluvial plain and the alluvial and lacustrine plain (Su et al. 2020). The multi-layer structure area includes phreatic aquifer, the upper confined aquifer, and the lower confined aquifer from top down. The thickness of the phreatic aquifer is thick in the south and thin in the north. The thickness of the phreatic aquifer is thick in the center of the plain and becomes thinner towards east and west. The phreatic aquifer is mainly composed of fine sand, silt, and sand gravel. The water abundance of the phreatic aquifer is less than 1000 m<sup>3</sup>/d. The irrigation water of the Yellow River is the main recharge source of the phreatic groundwater. As a traditional irrigation area with an irrigation history of 2000 years, the leakage of the Yellow River diversion canals and irrigation infiltration recharge account for more than 70% of the total recharge in the area (Qian et al. 2012, 2013, 2014). Under the influence of topography, geomorphology, hydrogeological conditions, and other factors, the lateral discharge to the Yellow River has become one of the ways for groundwater discharge in addition to artificial abstraction and groundwater evaporation.

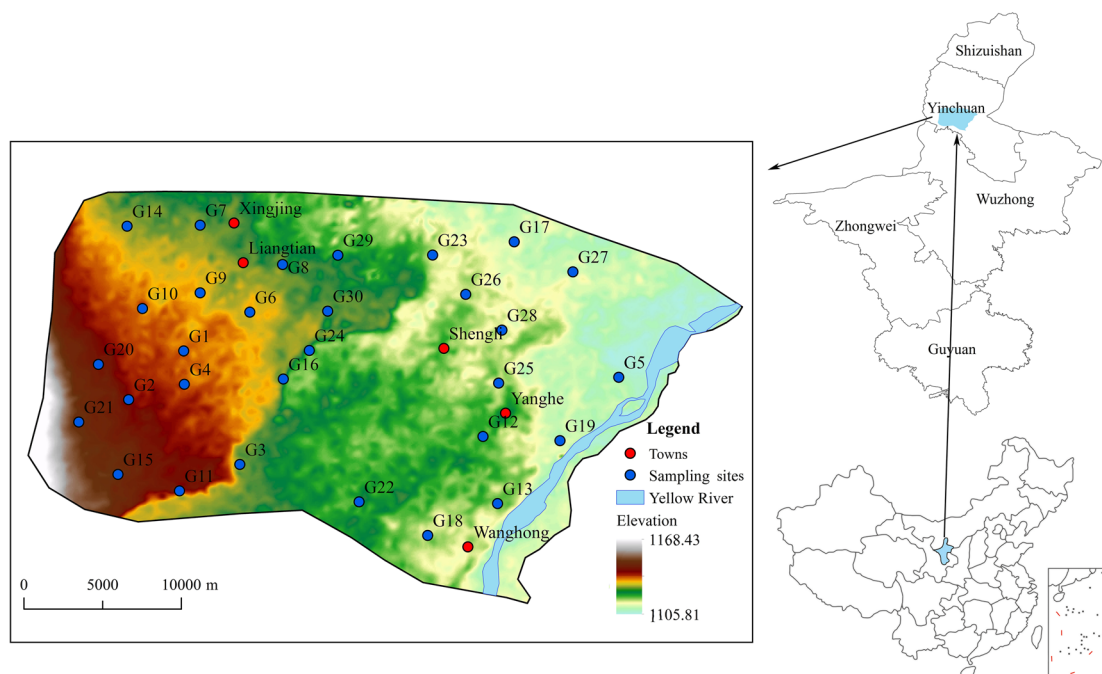


**Fig. 1** Geographical locations of the study area and sampling sites



Fig. 2 Zoning map of aquifer structure in Yinchuan Plain

## Material and Methods

### Sample Collection and Analysis

In the study, a total of sixty groundwater samples were collected from the phreatic aquifer in March (dry season) and July (wet season) in 2018 (30 in March and 30 in July). All groundwater samples were tested in the laboratory of Ningxia Institute of Land and Resources Investigation and Monitoring. Before collection, the wells were kept pumping for 10 to 15 min. When sampling, all samples were collected in white plastic bottles. The bottles were rinsed and washed 2 or 3 times thoroughly with the groundwater to be sampled before sampling. During the sampling process, the coordinates of the sampling points were recorded by a portable GPS.

The physicochemical parameters analyzed for each water sample include water temperature (T), pH, chemical oxygen demand (COD), dissolved total solids (TDS), total hardness (TH), major ions, and some trace elements. The major

cations include  $\text{Ca}^{2+}$ ,  $\text{Mg}^{2+}$ ,  $\text{Na}^+$ ,  $\text{K}^+$ , and  $\text{NH}_4\text{-N}$ , and the anions include  $\text{HCO}_3^-$ ,  $\text{Cl}^-$ ,  $\text{SO}_4^{2-}$ , and  $\text{NO}_3\text{-N}$ . Total iron (TFe), Mn, free  $\text{CO}_2$ ,  $\text{F}^-$ ,  $\text{PO}_4^{3-}$ , and As in groundwater samples were also determined. The temperature and pH were measured in the field by a pre-calibrated portable Hanna pH meter with an accuracy of 0.1 °C and 0.02 pH. The collection, preservation, and transportation of samples were processed according to national standards, and the preservation and testing of water samples were carried out in accordance with the methods stipulated in the Standards for drinking water quality (Ministry of Health of the PRC, Standardization Administration of the PRC 2006). Among the analyzed parameters,  $\text{Na}^+$  and  $\text{K}^+$  were measured using a flame photometer (Systronics k-1/mk-III).  $\text{HCO}_3^-$ ,  $\text{Cl}^-$ ,  $\text{SO}_4^{2-}$ , and  $\text{NH}_4\text{-N}$  were measured using titrimetric method. TDS was measured by drying and weighing method, and  $\text{Ca}^{2+}$ ,  $\text{Mg}^{2+}$ , and TH were measured by EDTA titrimetric method. The ion chromatography method was used to determine the concentration of  $\text{NO}_3\text{-N}$ . (Wu et al. 2017). The concentrations of TFe and Mn were determined by plasma emission spectrometry methods (Rice et al. 2017). The ion-selective electrode method and hydride generation atomic fluorescence spectrometry method were used to determine the  $\text{F}^-$  and As, respectively (Rice et al. 2017). In the study, duplication was introduced to ensure the accuracy of the analysis. After analysis, charge balance error percentage (CBE%) was introduced and only those with CBE% lower than 5% were used in the study.

### Correlation Analysis

Multivariate statistical techniques are widely used in groundwater hydrochemical analysis (Wu et al. 2014, 2020). Correlation analysis was used to determine the correlations between each pair of the physicochemical. In the study, the correlation of variables was determined by Pearson correlation coefficient, which is defined as the quotient of covariance and standard deviation between two variables (Eq. 1):

$$r = \frac{\sum_{i=1}^n (X_i - \bar{X})(Y_i - \bar{Y})}{\sqrt{\sum_{i=1}^n (X_i - \bar{X})^2} \sqrt{\sum_{i=1}^n (Y_i - \bar{Y})^2}} \quad (1)$$

The value of  $r$  ranges between  $-1$  and  $1$ . The closer the value is to  $1$ , the greater the positive correlation between the variables. On the contrary, the closer the value is to  $-1$ , the greater the negative correlation between the variables. The correlation coefficient of  $0$  indicates that the two variables are not correlated. Pearson correlation coefficients were calculated with SPSS 25.0 for Windows (Li et al. 2013).

## Kriging Interpolation

Kriging interpolation is the best interpolation method of analyzing spatial self-covariance. It can effectively transform the discrete point information into continuous area information (Hu and Shu 2015). Kriging is widely used in groundwater simulation, soil mapping, and other fields (Bargaoui and Chebbi 2009). It considers the variation distribution of spatial attributes in the spatial position, determines the distance range that has influence on the value of a point to be estimated, and then uses the sampling points in this range to estimate the attribute value of the point to be estimated. Mathematically, this method can provide an optimal linear unbiased estimation (the definite value at a certain point) for the object studied. According to the measured data, after the structural analysis, a weight coefficient is given by the data of the known points, and the weighted average is carried out to obtain the value of the point to be estimated in the range (Guagliardi et al. 2012; Li et al. 2014). The equations are as follows (Eqs. 2 and 3):

$$Z^*(x_0) = \sum_{i=1}^N \lambda_i Z(x_i) \quad (2)$$

$$\sum_{i=1}^N \lambda_i r(x_i, x_j) + u = r(x_i, x_0), \quad \sum_{i=1}^N \lambda_i = 1 \quad (3)$$

where,  $x_0$  denotes the point to be estimated, the  $Z^*(x_0)$  is the estimated value of  $x_0$ ,  $\lambda_i$  is the weight coefficient,  $x_i$  is the known points,  $Z(x_i)$  is the measured data,  $r(x_i, x_j)$  is a variation function, and  $u$  is a Lagrange multiplier.

According to Eq. 3 and the transformation relations of variance function, the theoretical variance  $\sigma^2$  can be calculated as per Eq. 4 (Guagliardi et al. 2012).

$$\sigma^2 = \sum_{i=1}^N \lambda_i r(x_i, x_0) + u \quad (4)$$

To judge the accuracy of the interpolation, an ideal variance  $\sigma_0^2$  can be determined, and the difference between  $\sigma_0^2$  and  $\sigma^2$  can be used to judge the accuracy of the interpolation. If the difference is unacceptable, the number of interpolation points can be modified until the difference between  $\sigma_0^2$  and  $\sigma^2$  becomes acceptable. In this study, the surfer 13 software is used to generate the ordinary Kriging interpolation, and 3556 nodes were generated in the X direction, while 2595 nodes were selected in the Y direction.

## Results and Discussion

### Physicochemical Characteristics of Groundwater

Table 1 shows the statistical results of the groundwater chemical compositions in the dry and wet seasons. As shown in Table 1, pH varied in the ranges of 7.05–8.10 in the wet season, and ranged from 7.42 to 8.27 in the dry season. All groundwater samples are weakly alkaline. The total hardness (TH) of the aquifers, which reflects the total concentration of  $\text{Ca}^{2+}$  and  $\text{Mg}^{2+}$  and the soap neutralizing power of a water sample (Cotruvo and Bartram 2009; Lidia 2014; Wu et al. 2017), ranged from 159.96 to 1254.57 mg/L in the dry season, and varied in the range of 254.93–1244.55 mg/L in the wet season. In this study, the TH values of 20 samples in the wet season and 21 samples in the dry season exceed the national guidelines (General Administration of Quality Supervision, Inspection & Quarantine of China and Standardization Administration of China 2017). The total dissolved solids (TDS) in the study area ranged between 315.76 and 2174.24 mg/L in the dry season, and ranged from 329.47 to 2194.48 mg/L in the wet season. According to the mean TDS values in the dry and wet seasons, phreatic groundwater is brackish water.

Values of  $\text{Ca}^{2+}$ ,  $\text{Mg}^{2+}$ ,  $\text{Na}^+$ , and  $\text{K}^+$  varied in the range of 34.03–172.17 mg/L, 18.21–200.31 mg/L, 22.0–329.6 mg/L, and 2–17 mg/L, respectively, in the dry season, and varied in the range of 44.04–172.17 mg/L, 31.56–213.66 mg/L, 20.8–612.8 mg/L, and 3–22 mg/L in the wet season, respectively. The relative abundance of the major cations in the sampled groundwater is in the order of  $\text{Na}^+ > \text{Mg}^{2+} > \text{Ca}^{2+} > \text{K}^+$  according to the average concentration expressed in mmol/L. Among the cations,  $\text{Na}^+$  has the highest mean value (157.89 mg/L), and one sample in the wet season has very high  $\text{Na}^+$  concentration of 612.8, which is significantly higher than the acceptable limit of 200 mg/L specified in the drinking water standard of China (General Administration of Quality Supervision, Inspection & Quarantine of China and Standardization Administration of China 2017). Some studies have shown that sewage irrigation may be responsible for the high content of  $\text{Na}^+$  in groundwater (Wu et al. 2013, 2017). However, in the present study, intense groundwater evaporation is believed to be the main reason for the high concentration of  $\text{Na}^+$  in phreatic groundwater, because the

**Table 1** Statistical analyses of chemical parameters (units for all parameters are mg/L except pH)

Indices	Dry season			Wet season			Overall mean	National standards	NSBL
	Minimum	Maximum	Mean	Minimum	Maximum	Mean			
pH	7.42	8.27	7.66	7.05	8.10	7.42	7.54	6.5–8.5	0
TH	159.96	1254.57	580.99	254.93	1244.55	591.31	586.15	450	41
COD	0.78	3.24	1.65	0.56	4.85	1.15	1.40	3	3
TDS	315.76	2174.24	1045.51	329.47	2194.48	1080.54	1063.02	1000	27
Na <sup>+</sup>	22.0	329.6	153.71	20.8	612.8	162.05	157.89	200	11
K <sup>+</sup>	2	17	5.17	3	22	5.68	5.43	–	–
Ca <sup>2+</sup>	34.04	172.17	97.85	44.04	172.17	98.10	97.97	–	–
Mg <sup>2+</sup>	18.21	200.31	81.76	31.56	213.66	84.13	82.95	–	–
Cl <sup>-</sup>	33.16	356.27	161.552	33.61	423.49	169.62	165.59	250	12
SO <sub>4</sub> <sup>2-</sup>	48.92	769.82	294.31	60.95	913.65	307.58	300.95	250	27
HCO <sub>3</sub> <sup>-</sup>	28.23	689.33	428.97	210.08	761.54	449.7	439.34	–	–
CO <sub>2</sub>	8.26	24.77	13.62	4.13	16.51	12.38	13.002	–	–
NO <sub>3</sub> -N	0	94.92	8.80	0	96.05	6.866	7.84	20	6
NH <sub>4</sub> -N	0	5.44	0.51	0	4.66	0.35	0.46	0.5	10
PO <sub>4</sub> <sup>3-</sup>	0	0.04	0.0067	0	0.05	0.0046	0.0057	–	–
F <sup>-</sup>	0.03	1.10	0.404	0.10	1.8	0.48	0.442	1	4
As	0	0.029	0.0016	0	0.0048	0.0013	0.0014	0.01	2
Mn	0.003	1.038	0.245	0.002	1.114	0.29	0.269	0.1	30
Fe	0	7.4	1.17	0.01	4.84	1.13	1.14	0.3	19

The number of samples beyond the standard limits (the national standards were referenced first for the calculation of NSBL)

water level depth in the study area is very small and the evaporation rate is very high. The value of K<sup>+</sup> is very low, with a maximum of 5.43 mg/L, probably as a result of the weak mobility due to biological activity (Brunner and Baccini 1992; Wu et al. 2017). For anions, the overall mean concentrations of Cl<sup>-</sup>, SO<sub>4</sub><sup>2-</sup>, and HCO<sub>3</sub><sup>-</sup> are 165.59 mg/L, 300.95 mg/L, and 439.34 mg/L, respectively. The major anions, expressed in mmol/L, are in the order HCO<sub>3</sub><sup>-</sup> > Cl<sup>-</sup> > SO<sub>4</sub><sup>2-</sup>. HCO<sub>3</sub><sup>-</sup>, Ca<sup>2+</sup>, and Mg<sup>2+</sup> are the main ions in the study area, which may be due to the dissolution of calcite (CaCO<sub>3</sub>) and dolomite (CaMg(CO<sub>3</sub>)<sub>2</sub>) in the study area. The overall mean value of SO<sub>4</sub><sup>2-</sup> is 300.95 mg/L, and the maximum concentrations of it in the dry and wet and seasons are 769.82 and 913.65 mg/L, respectively, both of which far exceed the national standard for drinking water quality (General Administration of Quality Supervision, Inspection & Quarantine of China and Standardization Administration of China 2017).

Human activities have a strong impact on the quality of groundwater. The concentrations of NO<sub>3</sub>-N and NH<sub>4</sub>-N in the study area are relatively high, ranging from 0–94.92 mg/L and 0–5.44 mg/L, respectively, in the dry season, and 0–96.05 mg/L and 0–4.66 mg/L in the wet season, respectively. Among them, the concentration of NO<sub>3</sub>-N in 5 samples in the dry season and 1 sample in the wet season exceeds the national standard (20 mg/L). In both the dry and wet seasons, the concentration of NH<sub>4</sub>-N in 5 samples

exceeds the national standard (0.5 mg/L), respectively. The high concentration of NO<sub>3</sub>-N and NH<sub>4</sub>-N indicates the industrial and agricultural pollution in the study area. The concentration of F<sup>-</sup> in the study area is in the range of 0.03–1.10 mg/L in the dry season and 0.10–1.80 mg/L in the wet season, and the overall mean concentration is 0.442 mg/L. The concentration of F<sup>-</sup> in the study area is low, and only 4 samples exceed the national drinking water standard (1.0 mg/L).

The iron and manganese pollution in the study area is significant. The iron concentration is in the range of 0–7.4 mg/L and 0.01–4.84 mg/L in the dry and wet seasons, respectively. The mean concentrations of iron in the dry and wet seasons are 1.17 and 1.13 mg/L, respectively, which are much higher than the national drinking water standard of China (0.3 mg/L). The Mn concentration is in the range of 0.003–1.038 mg/L and 0.002–1.114 mg/L in the dry and wet seasons, respectively. The results show that half of the water samples collected have higher Mn concentration than the national drinking water standard, which indicates the wide distribution of manganese pollution. In this study, the As concentration ranges from 0 to 0.029 mg/L in the dry season, and from 0 to 0.0048 mg/L in the wet season. The average concentration of As is 0.0016 mg/L in the dry season and 0.0014 mg/L in the wet season. As content in the dry season has two excessive points, but for most samples, arsenic content in the wet season exceeds the dry season, and the

As content is quite different between the dry season and the wet season. It indicates that the concentration of As in the phreatic aquifer is significantly affected by the season, and it may be related to the climate, recharge, and discharge of the groundwater as well as human irrigation activities. The average annual precipitation in the area is 182.6 mm; therefore, the Yellow river introduced into the channels for irrigation may be the secondary source of Arsenic. The As level in the water of the upper reaches of the Yellow river ranged for 0.0023–0.0104 mg/L (Tian et al. 2017), which is higher than the average arsenic concentration in the study area. In addition, the study area has intense agricultural activities, and nitrogen fertilizer is the most used fertilizer followed by compound fertilizer, phosphate fertilizer, and potash fertilizer. Besides, hexazole alcohol, fluoramide, triadimefon, and other pesticides are also used in agriculture in the study area, which may be the causes of groundwater contamination in the study area.

The averages of all the elements in the study area show only slight changes in the dry and wet seasons. It indicates that the hydrogeological environment and hydrochemical processes in the study area are basically the same in both seasons. The contents of  $\text{Na}^+$ ,  $\text{K}^+$ ,  $\text{Ca}^{2+}$ ,  $\text{Mg}^{2+}$ ,  $\text{Cl}^-$ ,  $\text{SO}_4^{2-}$ ,  $\text{HCO}_3^-$ ,  $\text{F}^-$ , and Mn in the wet season are slightly higher than those in the dry season. This indicates that the leaching of irrigation water and rainfall during the wet seasons can introduce more soluble salts into groundwater. The infiltration of surface water or rainwater can also elevate the groundwater level, resulting in more groundwater evaporation and increasing their concentrations. In addition, the changes of hydrodynamics can also accelerate the dissolution of minerals such as carbonates and gypsum, increasing the concentrations of major ions. On the contrary, the

contents of  $\text{NO}_3\text{-N}$ ,  $\text{NH}_4\text{-N}$ ,  $\text{PO}_4^{3-}$ , As, and Fe in the wet season are slightly lower than those in the dry season, indicating that the dilution effect of irrigation water and rainfall on these elements or ions is greater than the evaporation effect.

Gibbs diagram is usually used to judge the natural evolution of surface water and the origin of ions, and it has also been widely used in the study of groundwater chemistry in recent years (He and Li 2020a). Gibbs diagrams classified the mechanisms which control the chemical properties of major dissolved salts in water into three types (Li et al. 2012). As shown in Fig. 3, most of the samples are plotted in rock dominance zone, which suggests that water–rock interaction plays an important role in the chemical evolution of groundwater. Rock weathering and water–rock interactions control the hydrochemical changes of groundwater in the study area. In addition, some points are plotted in the evaporation dominance zone, which may be attributed to the shallow depth and intense evaporation of unconfined groundwater in the Yinchuan Plain. The high groundwater evaporation may lead to the enrichment of As in phreatic groundwater.

In this study, Piper diagram (Piper 1953) was used to study the hydrochemical types in the study area (Fig. 4). Figure 4 shows that in the cationic triangle, most of the samples belong to no dominant type, and a few of them belong to sodium type, which indicates that the proportion of cations in groundwater in the study area is similar and belongs to mixed water. In the anionic triangle, some of the samples are located in the zone of no dominant type, which belongs to mixed water, and some of the samples are located in E region, which belongs to bicarbonate type. The Piper diagram shows that the main hydrochemical type in the study

**Fig. 3** Mechanisms controlling groundwater evolution based on Gibbs diagram

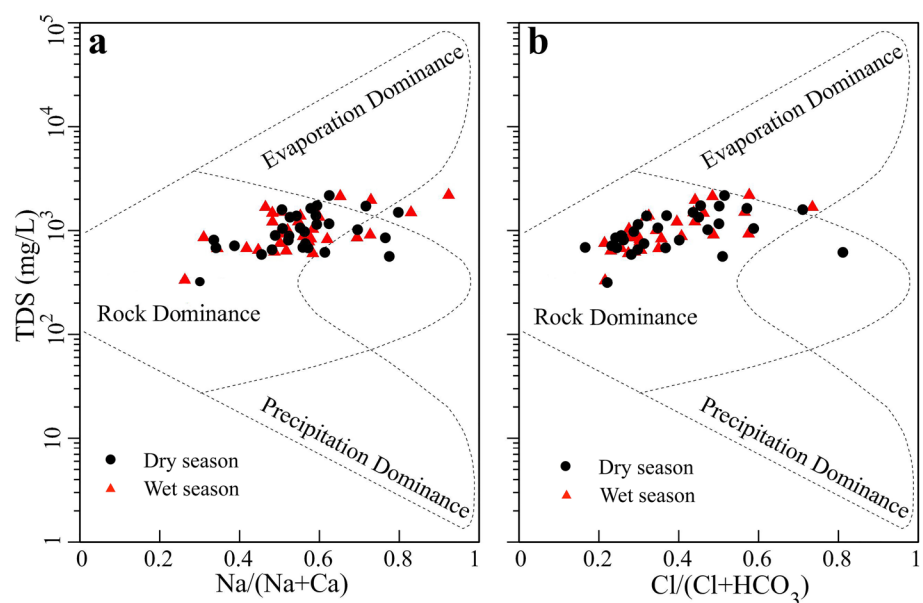
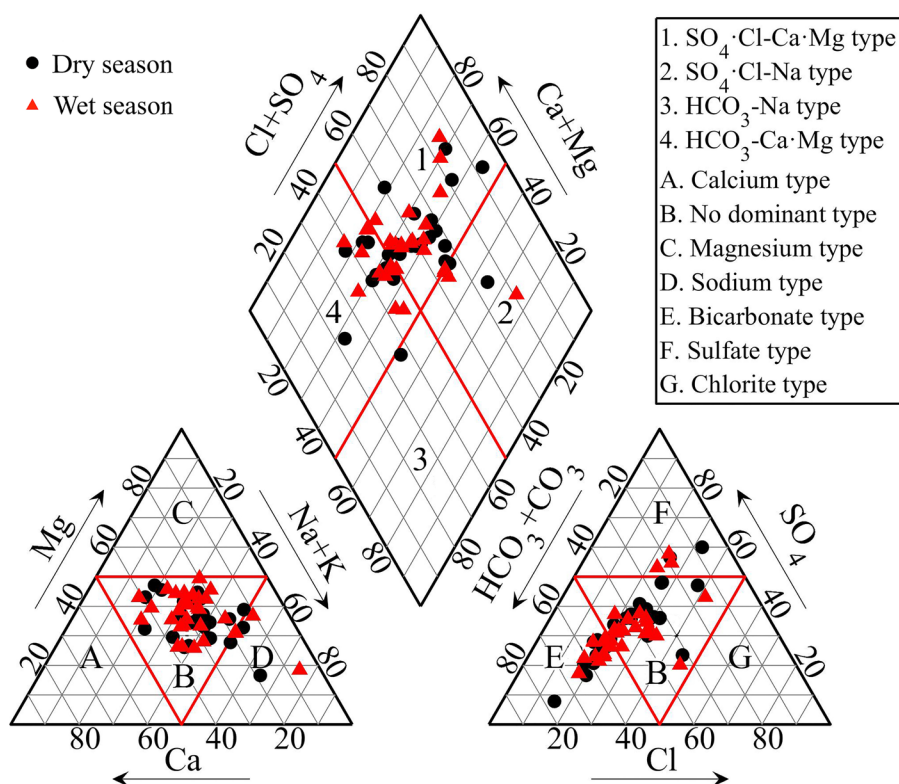


**Fig. 4** Hydrochemical types of groundwater in the study area based on Piper diagram



area is  $\text{SO}_4 \cdot \text{Cl} \cdot \text{Ca} \cdot \text{Mg}$  type, followed by  $\text{HCO}_3^- \cdot \text{Ca} \cdot \text{Mg}$  type in both seasons. The  $\text{Cl}^-$  and  $\text{SO}_4^{2-}$  type water is mainly the result of progressive salinization (Li et al. 2016), which comes from rock weathering and evaporation. The calcium carbonate type water mainly comes from the dissolution of carbonate. In this study, mixed  $\text{SO}_4 \cdot \text{HCO}_3^- \cdot \text{Ca} \cdot \text{Mg}$  type water may be due to mineral dissolution and strong evaporation. The dissociation of dolomite adds  $\text{Ca}^{2+}$ ,  $\text{HCO}_3^-$ , and  $\text{Mg}^{2+}$  into the solution, and the dissolution of calcite releases  $\text{Ca}^{2+}$  and  $\text{HCO}_3^-$  into the water (Abdalla and Al-Abri 2013; Li et al. 2016).

A large amount of dissolvable minerals and salts occurs in the sediments, which is the results of parent rock weathering. The soluble salts will enter groundwater along with the infiltration of irrigation water and precipitation (Li et al. 2016; He and Li 2020b). This process is classified as direct impacts of human activities by Li (2014). The impacts of human activities on the chemical compositions of groundwater can be divided into two categories: direct impacts and indirect impacts (Li 2014). Direct impacts of human activities are those that directly alter the contents of groundwater chemical compositions. On the contrary, indirect impacts do not alter the contents of groundwater chemical compositions directly, but they can indirectly influence the contents of groundwater chemical compositions by altering hydrodynamic conditions that may accelerate water–rock interaction processes and change groundwater evaporating intensity (Li 2016; Li et al. 2016, 2017).

### Groundwater Geochemical Processes Revealed by Correlation Analysis

The correlation of chemical elements in groundwater can help to understand the main hydrogeochemical processes that control the hydrochemical characteristics. The correlation analysis of the main hydrochemical elements in the study area was carried out (Tables 2 and 3).

Most of the groundwater physicochemical indices have a high correlation between each other in both seasons, but the correlation among the elements in the wet season are generally higher than that in the dry season. The correlation coefficients among TH, TDS,  $\text{Mg}^{2+}$ ,  $\text{Na}^+$ ,  $\text{SO}_4^{2-}$ , and  $\text{NO}_3^- \text{-N}$  in the wet season are very close to those in the dry season, which indicates that these indices are influenced by similar factors in both seasons and the influencing degrees to these indices are similar. The correlations among pH,  $\text{NH}_4^- \text{-N}$ , F,  $\text{PO}_4^{3-}$ , COD, and As show significant difference in the two seasons, because these indices may be influenced by different factors in the two seasons. For example, the content of COD is greatly affected by surface water recharge. In the dry season and wet season, the surface water recharging to groundwater has changed (Ji et al. 2020), which will alter the concentration of COD in groundwater, inducing the big change of the correlation coefficients between COD and other indices. The content of  $\text{PO}_4^{3-}$  in groundwater is strongly affected by human factors. In the study area, human activities are more intense



**Table 2** Correlation analysis of sample points in the dry season (March)

	pH	TH	TDS	Ca <sup>2+</sup>	Mg <sup>2+</sup>	K <sup>+</sup>	Na <sup>+</sup>	Cl <sup>-</sup>	SO <sub>4</sub> <sup>2-</sup>	HCO <sub>3</sub> <sup>-</sup>	NO <sub>3</sub> <sup>-</sup>	NH <sub>4</sub> <sup>+</sup>	Fe	F	PO <sub>4</sub> <sup>3-</sup>	Mn	As
pH	1																
TH	-0.535**	1															
TDS	-0.599**	0.942**	1														
Ca <sup>2+</sup>	-0.389*	0.874**	0.781**	1													
Mg <sup>2+</sup>	-0.559**	0.954**	0.926**	0.690**	1												
K <sup>+</sup>	-0.390*	0.239	0.198	0.128	0.279	1											
Na <sup>+</sup>	-0.580**	0.744**	0.920**	0.554**	0.770**	0.108	1										
Cl <sup>-</sup>	-0.484**	0.814**	0.906**	0.749**	0.754**	0.102	0.853**	1									
SO <sub>4</sub> <sup>2-</sup>	-0.541**	0.880**	0.937**	0.701**	0.881**	0.179	0.837**	0.832**	1								
HCO <sub>3</sub> <sup>-</sup>	-0.341	0.476**	0.452*	0.362*	0.488**	0.126	0.422*	0.287	0.176	1							
NO <sub>3</sub> <sup>-</sup>	-0.267	0.502**	0.426*	0.394*	0.506**	0.374*	0.340	0.235	0.460*	-0.011	1						
NH <sub>4</sub> <sup>+</sup>	-0.244	-0.145	-0.133	-0.235	-0.070	0.130	-0.100	-0.083	-0.209	0.097	-0.060	1					
Fe	-0.139	0.151	0.151	0.229	0.084	-0.121	0.083	0.221	0.033	0.303	-0.269	0.181	1				
F	-0.343	0.111	0.142	-0.041	0.190	0.299	0.174	0.063	0.169	-0.165	0.379*	0.301	-0.172	1			
PO <sub>4</sub> <sup>3-</sup>	0.156	-0.270	-0.345	-0.172	-0.298	-0.094	-0.384*	-0.341	-0.315	-0.242	-0.100	0.085	0.139	0.265	1		
Mn	-0.276	0.395*	0.409*	0.275	0.421*	-0.057	0.391*	0.371*	0.254	0.404*	0.257	0.269	0.570**	0.214	0.145	1	
As	0.096	-0.063	-0.063	-0.139	-0.008	0.059	-0.031	-0.055	-0.176	0.238	-0.137	0.524**	0.175	0.137	0.351	0.433*	1

\*\*Significance at the 0.01 level

\*Significance at the 0.05 level

**Table 3** Correlation analysis of sample points in the wet season (July)

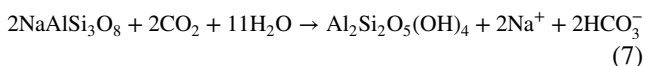
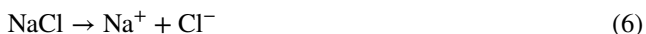
	pH	TH	TDS	Ca <sup>2+</sup>	Mg <sup>2+</sup>	K <sup>+</sup>	Na <sup>+</sup>	Cl <sup>-</sup>	SO <sub>4</sub> <sup>2-</sup>	HCO <sub>3</sub> <sup>-</sup>	NO <sub>3</sub> <sup>-</sup>	NH <sub>4</sub> <sup>+</sup>	Fe	F	PO <sub>4</sub> <sup>3-</sup>	Mn	As
pH	1																
TH	-0.373*	1															
TDS	0.141	0.762**	1														
Ca <sup>2+</sup>	-0.512**	0.797**	0.468**	1													
Mg <sup>2+</sup>	-0.232	0.941**	0.795**	0.546**	1												
K <sup>+</sup>	0.162	0.195	0.200	0.047	0.243	1											
Na <sup>+</sup>	0.472**	0.347	0.868**	0.045	0.456*	0.130	1										
Cl <sup>-</sup>	0.130	0.694**	0.872**	0.557**	0.651**	0.101	0.717**	1									
SO <sub>4</sub> <sup>2-</sup>	0.232	0.688**	0.951**	0.381*	0.741**	0.236	0.841**	0.774**	1								
HCO <sub>3</sub> <sup>-</sup>	-0.278	0.408*	0.411*	0.237	0.434*	-0.035	0.334	0.259	0.169	1							
NO <sub>3</sub> <sup>-</sup>	-0.092	0.522**	0.377*	0.246	0.587**	0.334	0.183	0.160	0.439*	-0.068	1						
NH <sub>4</sub> <sup>+</sup>	0.070	-0.074	-0.012	-0.065	-0.067	0.086	0.032	0.019	-0.087	0.167	-0.075	1					
Fe	-0.195	0.199	0.153	0.287	0.115	-0.115	0.059	0.184	-0.005	0.525**	-0.247	0.231	1				
F	0.474**	-0.066	0.307	-0.355	0.107	0.318	0.519**	0.064	0.391*	-0.013	0.294	0.074	-0.327	1			
PO <sub>4</sub> <sup>3-</sup>	0.086	-0.214	-0.294	-0.135	-0.221	-0.029	-0.277	-0.297	-0.222	-0.220	-0.101	-0.001	-0.165	-0.016	1		
Mn	-0.095	0.419*	0.334	0.302	0.413*	0.077	0.189	0.265	0.179	0.532**	0.291	0.270	0.607**	0.004	-0.006	1	
As	-0.038	0.056	-0.019	-0.020	0.089	0.137	-0.097	0.132	0.078	-0.415*	-0.041	0.021	-0.279	0.075	-0.031	-0.318	1

\*\*Significance at the 0.01 level

\*Significance at the 0.05 level

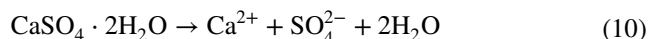
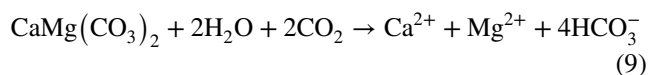
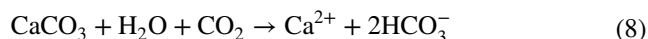
and extensive in the wet season than in the dry season, so the correlation coefficients of  $\text{PO}_4^{3-}$  with other indices are different in the two seasons. Significant correlations of TDS with  $\text{SO}_4^{2-}$ ,  $\text{Mg}^{2+}$ ,  $\text{Ca}^{2+}$ ,  $\text{Na}^+$ , and  $\text{Cl}^-$  are observed in both seasons, which indicates that these ions are the main components of TDS and rock weathering, and are playing an important role in the groundwater hydrochemical evolution of the study area.

To discuss more specifically, the correlation between  $\text{Na}^+$  and  $\text{SO}_4^{2-}$  is high ( $r=0.837$  in the dry season and  $r=0.841$  in the wet season), and the correlation among  $\text{Na}^+$  and  $\text{Cl}^-$  is also high ( $r=0.853$  in the dry season and  $r=0.717$  in the wet season), which indicates that  $\text{Na}^+$  mainly comes from the dissolution of evaporates such as halite and mirabilite in the study area. Some of the plots are plotted along the 2:1 line, but some plots deviate from the 2:1 line (Fig. 5a), suggesting that some other factors are affecting the concentrations of  $\text{Na}^+$  and  $\text{SO}_4^{2-}$ . The linear relationship between  $\text{Na}^+$  and  $\text{SO}_4^{2-}$  in the study area is  $y=0.399x+0.390$ . If  $\text{Na}^+$  and  $\text{Cl}^-$  come solely from dissolution of halite, the samples should be plotted along the 1:1 line (Fig. 5b). As shown in Fig. 5b, the plots deviate from the 1:1 line, and more  $\text{Na}^+$  is observed than  $\text{Cl}^-$ . The  $\text{Cl}^-$  and  $\text{Na}^+$  concentration conform to the fitting  $y=0.471x+1.494$ . This shows that halite dissolution is not the sole source of  $\text{Na}^+$ , but it plays a critical role in regulating the content of  $\text{Na}^+$ . In addition to the dissolution of evaporates mentioned above, cation exchange and silicate weathering may also contribute to the concentration of  $\text{Na}^+$  in the water. The chemical reactions mentioned above can be expressed as follows.



$\text{Ca}^{2+}$  and  $\text{Mg}^{2+}$  display significant positive correlation with  $\text{SO}_4^{2-}$  and  $\text{HCO}_3^-$  as shown in Tables 2 and 3, indicating that they may have the same source in groundwater (Ren et al. 2021), such as weathering and dissolution of gypsum ( $\text{CaSO}_4 \cdot 2\text{H}_2\text{O}$ ), dolomite ( $\text{CaMg}(\text{CO}_3)_2$ ) and calcite ( $\text{CaCO}_3$ ). The dissolution of calcite and dolomite is expressed by Eqs. (8) and (9), respectively. The plots of  $\text{HCO}_3^-$  versus  $\text{Ca}^{2+} + \text{Mg}^{2+}$  (Fig. 5c) are mainly located in the area between the 2:1 line and 1:1 line, and the plot of  $\text{HCO}_3^-$  versus  $\text{Ca}^{2+}$  (Fig. 5d) is mainly situated below the 2:1 line, suggesting that dolomite and calcite are the sources of  $\text{Ca}^{2+}$  and  $\text{HCO}_3^-$  in the groundwater of the study area. However, they are not the sole factors affecting the

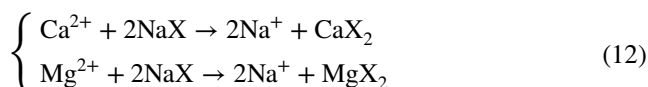
concentration of  $\text{Ca}^{2+}$ . The excess of  $\text{HCO}_3^-$  over  $\text{Ca}^{2+}$  in Fig. 5d reveals that cation exchange mentioned previously is an important process in the study area. Gypsum can be dissolved into water and forms  $\text{Ca}^{2+}$  and  $\text{SO}_4^{2-}$  in groundwater (Eq. 10). As shown in Fig. 5e, when the concentration of  $\text{Ca}^{2+}$  in groundwater in the study area is lower than 4 mmol/L, the relationship of  $\text{Ca}^{2+}$  versus  $\text{SO}_4^{2-}$  conforms generally to the 1:1 line, suggesting that gypsum dissolution is dominant in the study area. However, with the increase of  $\text{Ca}^{2+}$  concentration in groundwater, the relationship between  $\text{Ca}^{2+}$  and  $\text{SO}_4^{2-}$  no longer follows the 1:1 line and the plots deviate towards below the 1:1 line, indicating again that cation exchange is an important process regulating the concentration of  $\text{Ca}^{2+}$  in the study area.



In groundwater with high concentrations of  $\text{Ca}^{2+}$  and  $\text{Mg}^{2+}$ , cation exchange between  $\text{Ca}^{2+}/\text{Mg}^{2+}$  and  $\text{Na}^+$  may occur. The cation exchange results in the release of  $\text{Na}^+$  from the solid surface into groundwater and increases the concentration of  $\text{Na}^+$ . There is a strong correlation between  $\text{Na}^+$  and  $\text{Ca}^{2+}/\text{Mg}^{2+}$  in the dry season in the study area, while the correlation of  $\text{Na}^+$  with  $\text{Ca}^{2+}$  in the wet season is not significant. This indicates that cation exchanges of  $\text{Na}^+$  with  $\text{Ca}^{2+}/\text{Mg}^{2+}$  are strong in the dry season, while in the wet season, only cation exchange between  $\text{Na}^+$  and  $\text{Mg}^{2+}$  is strong. To further explain the cation exchange, two chloro-alkaline indices (CAI-1, CAI-2) were used in this study, which can be expressed by Eq. 11. When the value of CAI-1 and CAI-2 are negative, exchange between  $\text{Ca}^{2+}/\text{Mg}^{2+}$  in groundwater and  $\text{Na}^+$  from solid surface occurs (Eq. 12), while when both values are positive, the reverse process occurs. As shown in Fig. 5f, the values of CAI-1 and CAI-2 for the majority of the samples are negative, indicating that  $\text{Na}^+$  in the solid surface is exchanged by  $\text{Ca}^{2+}/\text{Mg}^{2+}$  in the groundwater. In this case, the  $\text{Ca}^{2+}/\text{Mg}^{2+}$  concentrations may be lowered and the concentration of  $\text{Na}^+$  is increased (Li et al. 2015; Ahmed et al. 2012).

$$\text{CAI} - 1 = \frac{\text{Cl}^- - (\text{Na}^+ + \text{K}^+)}{\text{Cl}^-} \quad (11)$$

$$\text{CAI} - 2 = \frac{\text{Cl}^- - (\text{Na}^+ + \text{K}^+)}{\text{HCO}_3^- + \text{SO}_4^{2-} + \text{CO}_3^{2-} + \text{NO}_3^-}$$



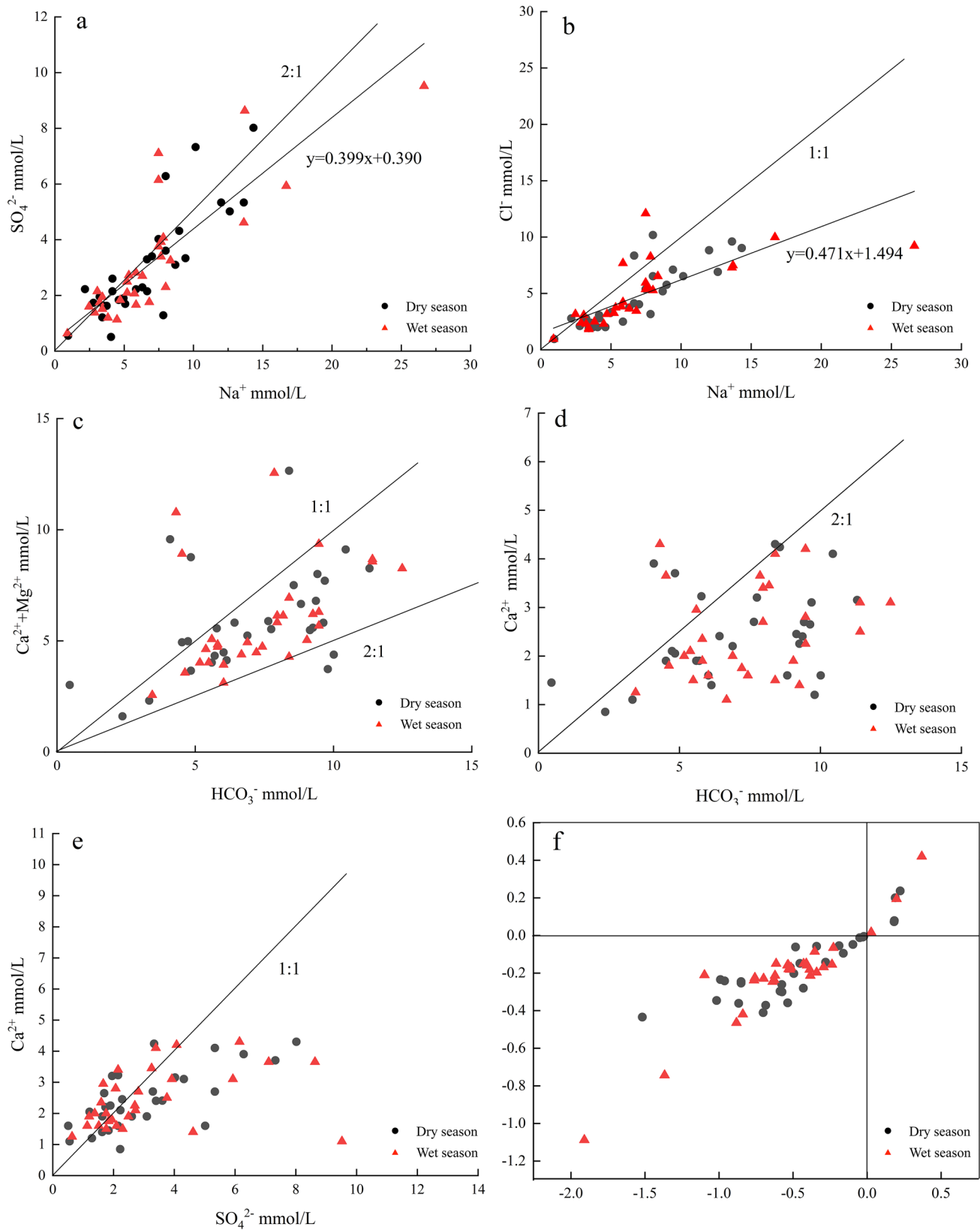
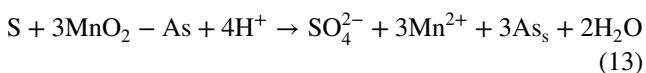


**Fig. 5** Binary ionic relation between **a**  $\text{Na}^+$  and  $\text{SO}_4^{2-}$ , **b**  $\text{Na}^+$  and  $\text{Cl}^-$ , **c**  $\text{HCO}_3^-$  and  $\text{Ca}^{2+} + \text{Mg}^{2+}$ , **d**  $\text{HCO}_3^-$  and  $\text{Ca}^{2+}$ , **e**  $\text{SO}_4^{2-}$  and  $\text{Ca}^{2+}$ , and **f** CAI of cation exchange

## Hydrochemical Environment for As Enrichment

The correlation analysis results show that the correlation of As with various elements is quite different in dry and wet periods. Significant positive correlations of As with  $\text{NH}_4^+$ ,  $\text{PO}_4^{3-}$ , and Mn (correlation coefficients are 0.524, 0.351, and 0.433, respectively) and a weak positive correlation between  $\text{HCO}_3^-$  and As (correlation coefficient is 0.238) in the dry season were observed. On the contrary, a strong negative correlation between As and  $\text{HCO}_3^-$  (correlation coefficient is  $-0.415$ ) and weak negative correlations of As with Fe, and Mn (correlation coefficients are  $-0.279$  and  $-0.318$ , respectively) were observed in the wet season.

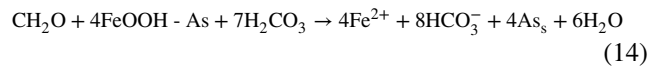
As oxidation, adsorption and desorption are common processes regulating the concentration of As in groundwater (Bian et al. 2015). In addition, the enrichment and transport of As in groundwater are also affected by surface water infiltration and human activities. Table 2 indicates that As has a high correlation with  $\text{PO}_4^{3-}$ , because arsenate and phosphate have similar chemical structures and properties (Duan 2016), resulting in competitive adsorption between phosphate and arsenate (Alam et al. 2016). The increase of phosphate in groundwater from agricultural activities will promote the desorption of arsenate, increasing the concentration of As in groundwater. Under weakly alkaline conditions,  $\text{NH}_4^+$  can promote the desorption of As adsorbed on the surface of iron and manganese hydroxides, increasing As concentration in groundwater. The reductive dissolution of arsenic-containing manganese oxides results in a positive correlation between Mn content and As (Eq. 13).



where  $\text{As}_s$  represents the As complexes in solution occurring as uncharged or negatively charged oxyanions.

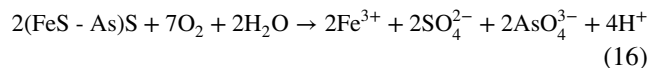
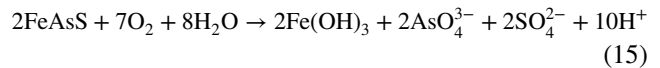
In addition, the strong correlation between As and  $\text{PO}_4^{3-}/\text{NH}_4^+\text{-N}$  indicates another possible source of As in groundwater, i.e., chemical fertilizers and organic wastes. The west and north of the study area are large zone of irrigated agricultural areas diverting from the Yellow River. Untreated chemical fertilizers and organic wastes are leached into phreatic groundwater. On the one hand, there may contain As in chemical fertilizers. On the other hand, the existence of organic wastes can promote desorption of As. These two ways may increase the content of As in groundwater.

Arsenite is absorbed and co-precipitated by calcite (Roman-Ross et al. 2006), so there is a significant negative correlation between As and bicarbonate when the concentration of bicarbonate is high. The negative correlation between As and bicarbonate may also be related to the oxidation of organic matter by microorganisms in the process of reducing hydroxide and releasing As at high temperature (Eq. 14).



where  $\text{As}_s$  is the As complexes in solution occurring as uncharged or negatively charged oxyanions C, and  $\text{CH}_2\text{O}$  represents organic matter.  $\text{FeOOH-As}$  denotes As adsorbed by ferric oxyhydroxide.

As and Fe often exist in the form of sulfides in groundwater, such as pyrite ( $\text{FeS-As}$ ) and arsenopyrite ( $\text{FeAsS}$ ) (Ahn 2012), and their dissolution in water can be expressed as follows (Duan 2016).



The increase of  $\text{Fe}^{3+}$  in local sewage will enhance As adsorption onto the iron hydroxide surface and form arsenate, that is, thus reducing the content of As in groundwater. This means  $\text{Fe}^{3+}$  should have a negative correlation with As. According to Eq. 14, the content of  $\text{Fe}^{2+}$  and that of As should have been positively correlated. However, the correlation analysis during the wet season shows that total Fe and As show a negative correlation. This indicates that  $\text{Fe}^{3+}$  is the main form of Fe in the study area to affect As content in the groundwater. Figure 6 is the conceptual model illustrating the hydrochemical processes driving As enrichment in groundwater.

## Temporal and Spatial Variation of As

In this study, the contour maps of As concentration and related ions ( $\text{HCO}_3^-$ ,  $\text{PO}_4^{3-}$ , Mn,  $\text{NH}_4^+$ ) are drawn by Kriging interpolation. Figure 7 shows the contour map of As concentration in the dry season (Fig. 7a) and wet season (Fig. 7b). The concentration difference between the two seasons is shown in Fig. 7c, which shows significant changes in the distribution of As in the phreatic groundwater in the dry season (March) and wet season (July). The content of As in groundwater is low in the dry period, and As is high in the north and southeast of the study area. However, As concentration in the wet season spreads westward compared with that in the dry season, and the As concentration in the groundwater increases in the wet season.

High As areas during the dry period are located in the north where canals are densely distributed and the areas near the Yellow River in the southeast. The closer to the surface water, the higher the content of As in groundwater can be. This indicates that the content of As in groundwater is mainly controlled by surface water. In the wet season, the Yellow River water is used for irrigation in agricultural irrigation areas, and the irrigation water diverted from the Yellow River becomes the main recharge source

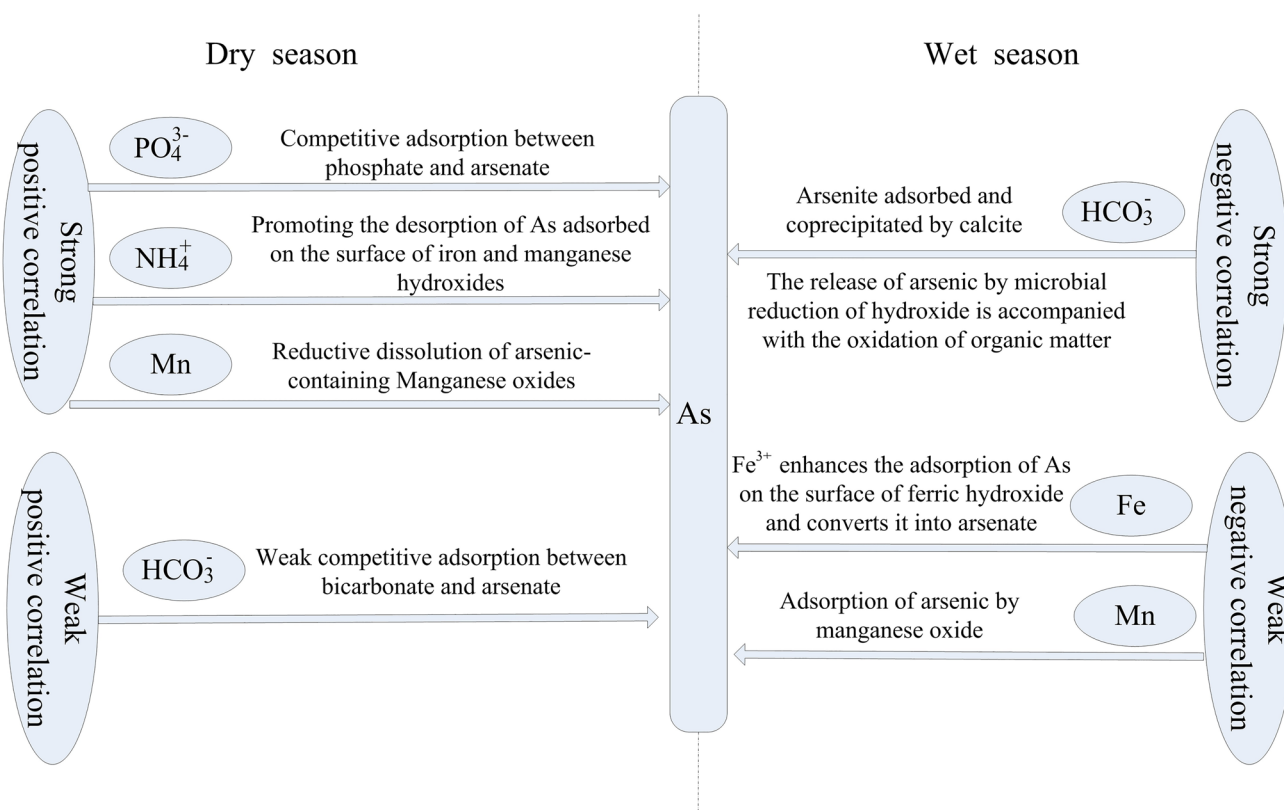


**Fig. 6** Conceptual diagram of the hydrochemical process driving As enrichment

of groundwater. The infiltration of irrigation water may lead to the increase of phosphate and nitrogen in groundwater. In addition, the infiltration of irrigation water changes the dynamic conditions of groundwater, which may promote or inhibit a series of water–rock interactions in the groundwater environment. This will increase the concentration of As in the wet season and extend As enrichment areas towards the agricultural irrigation areas in the west. The above discussion indicates that surface water infiltration may modify the subsurface environment and enhance the water–rock interactions, accelerating the release of As into groundwater.

At the same time, agricultural activities are strengthened in the wet season, which may also lead to an increase in As content in agricultural irrigation areas. Figure 7c shows that the changes of As content are small in the areas close to the surface water, while in the areas far away from surface water, the content of As varies greatly in the two season. This phenomenon is due to the fact that in the areas close to the Yellow River, the hydrochemical process in groundwater is mainly affected by the Yellow River water. The percolation of the Yellow River into subsurface area does not change significantly during the two seasons. Therefore, the As concentration in the two seasons does not change significantly in the near-river areas. However, in the far-river areas, the infiltration of surface water is completely different during

the two seasons. The infiltration of surface water is strong in the wet season and weak in the dry season. Therefore, As concentration in the far-river areas varies significantly. In addition, the human activities are more intense in the far-river areas than in the near-river areas, because more agricultural lands are located in the far-river areas.

Figure 8 shows the contour maps of  $\text{HCO}_3^-$ ,  $\text{PO}_4^{3-}$ , Mn, and  $\text{NH}_4\text{-N}$  that are significantly correlated with As during the dry season (Fig. 8a, c, e, g) and the wet season (Fig. 8b, d, f, h). As shown in Fig. 8,  $\text{HCO}_3^-$  shows an obvious seasonal effect, while that of  $\text{PO}_4^{3-}$  does not. The contours of concentration distribution of Mn and  $\text{NH}_4\text{-N}$  in the wet season and dry season are basically the same, respectively, suggesting that they have no seasonal variation. It can be seen from the Figs. 7 and 8 that the distributions of As content in the dry season are similar to that of Mn and  $\text{NH}_4\text{-N}$ , indicating that they may have the same influencing factors during the dry season. During the wet season, the contour of As concentration shows an opposite trend to that of  $\text{HCO}_3^-$ , which confirms the results of correlation analysis.

In the dry season, the infiltration of surface water and disturbance of human activities to groundwater is relatively smaller compared to those in the wet season. In the wet season, the reductive dissolution of manganese oxides containing As, accompanied by the competitive adsorption

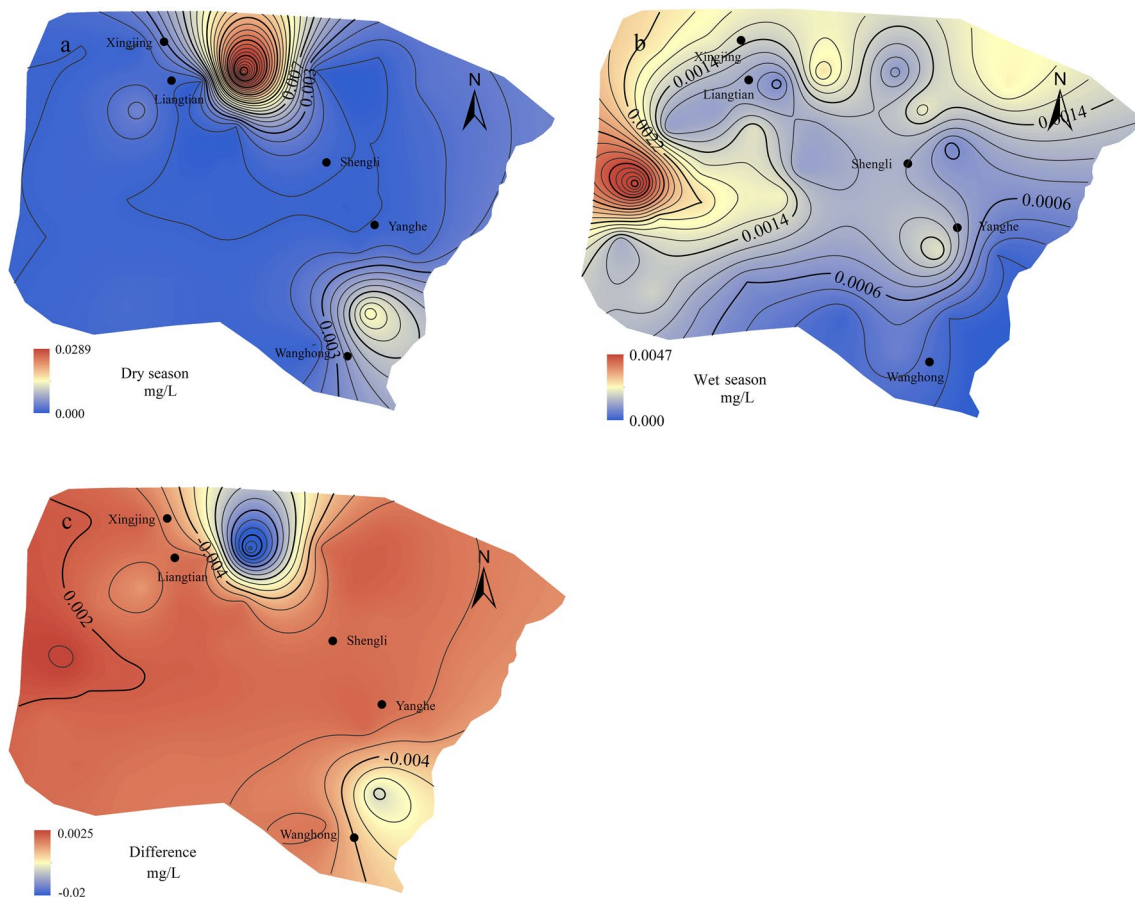


**Fig. 7** Contour maps of **a** As in the dry season, **b** As in the wet season, **c** difference between the dry and wet seasons

of phosphate, carbonate, and arsenate, affects significantly As content in groundwater during the wet season. However, the distribution of As is different from that of  $\text{NH}_4^+$  in the dry season. This shows that the effect of agricultural chemical fertilizers and organic wastes on the content of As in the dry wet season is weaker compared with the effect of surface water infiltration. This shows that the subsurface environment change caused by surface water infiltration is the dominant factor affecting As release into groundwater. In the wet season, the rise of oxygen in groundwater leads to the enhancement of oxidation in the subsurface areas.  $\text{Fe}^{2+}$  and  $\text{NH}_4^+$  are oxidized, and their controls on As content in groundwater is relatively weakened.  $\text{Fe}^{3+}$  becomes one of the main elements affecting the enrichment of As in aquifers in the wet season.

### Health risks of As

Exposure to As in drinking water can cause a series of diseases such as lung cancer, respiratory cancer, prostate cancer, high blood pressure, and diabetes (Lamm et al. 2018; Welch et al. 1982; Ahn et al. 2020; Wang et al. 2011;

Bräuner et al. 2014; He et al. 2020b). People exposed to high and medium levels of As have high rates of mortality and lung cancer (Khan et al. 2020). Zhao et al. (2014) conducted meta-analysis on the dose–response relationship between arsenic concentration in water and the risk of lung cancer. The results of analysis indicated that when As concentration in drinking water increased by 1  $\mu\text{g}/\text{L}$ , the risk of lung cancer would be increased by 0.07%–0.22%. In order to quantify the relationship between the incidence of lung cancer and As concentration in drinking water, Lamm et al. (2018) calculated the incidence of lung cancer and the concentration of arsenic in drinking water in American counties from 2009 to 2013 and established a linear model between the total lung cancer rate and the median value of As in drinking water (Fig. 9). Data sources of the linear model included USGS for arsenic exposure, NCI for lung cancer outcome, and CDC and US Census Bureau for covariates. To demonstrate the average situation of the risk in the study area, mean arsenic level was used to estimate the lung cancer risk in this study.

Line 1 represents the linear relationship of As with the total lung cancer when the median value of As is less than 25  $\mu\text{g}/\text{L}$ , and it satisfies  $y = -0.837x + 67.766$  ( $R^2 = 0.018$ ,

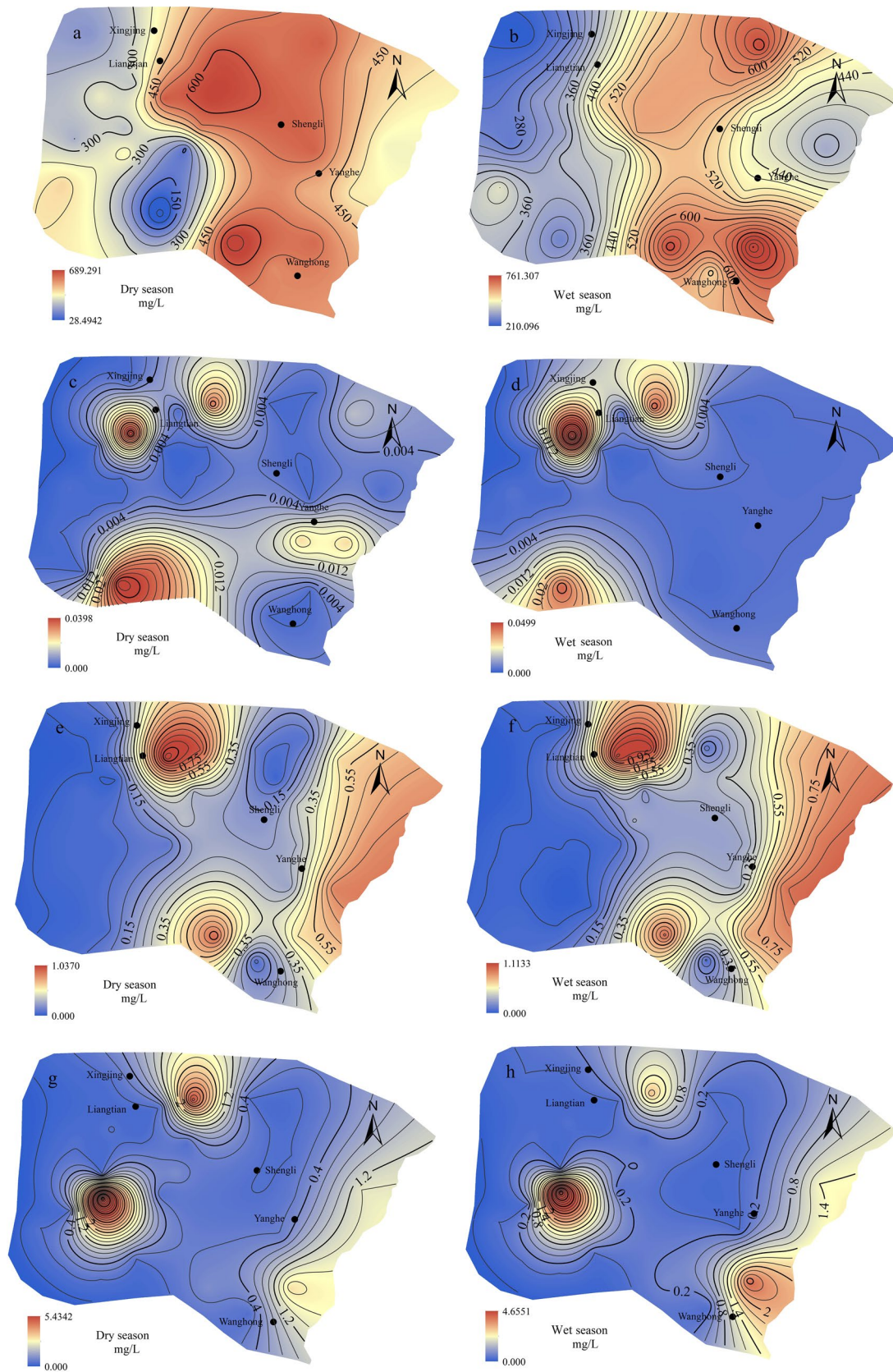


**Fig. 8** Contour maps of (a, b)  $\text{HCO}_3^-$ , (c, d)  $\text{PO}_4^{3-}$ , (e, f) Mn, and (g, h)  $\text{NH}_4^+$  in the dry season and wet season



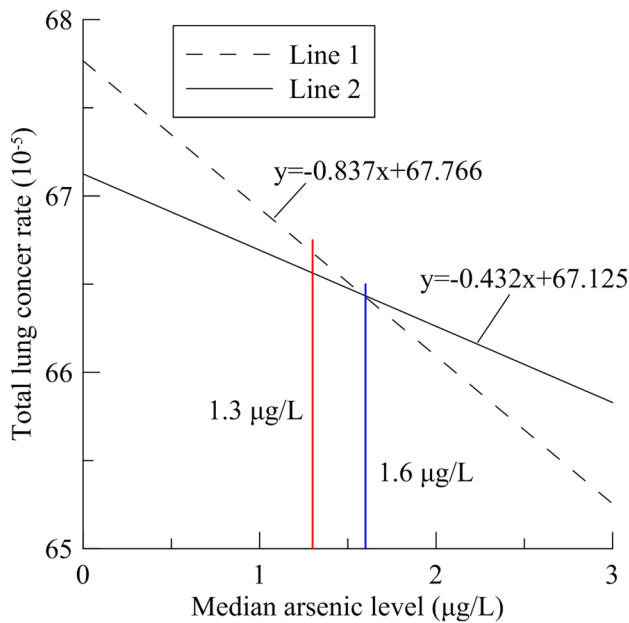


**Fig. 9** Linear relationship between As level ( $\mu\text{g/L}$ ) and the total lung cancer rate

$p < 0.001$ ). In this study, the mean value of As in the dry season is  $1.6 \mu\text{g/L}$ , and that in the wet season is  $1.3 \mu\text{g/L}$ , indicating a total lung cancer rate of  $66.43 \times 10^{-5}$  and  $66.68 \times 10^{-5}$  in the dry and wet seasons, respectively. This means around 66 out of 100 thousand persons may suffer from lung cancer due to drinking high As water. Line 2 is the revised relationship between the median value of As and the total lung cancer rate when the median value of As is lower than  $100 \mu\text{g/L}$ . The revised relationship fits  $y = -0.432x + 67.125$  ( $R^2 = 0.012$ ,  $p = 0.003$ ). Calculated from line 2, the total lung cancer rate of As exposure in the study area is  $66.43 \times 10^{-5}$  in the dry period and  $66.56 \times 10^{-5}$  in the wet season. Both relationships show that the total lung cancer rate of As exposure in the wet season is slightly higher than that in the dry season in the study area. The lung cancer risk is higher than the maximum acceptable level ( $1 \times 10^{-4}$ ). Thus, As treatment is required for drinking water in the study area.

Some existing measures can effectively control the industrial point source pollution of metals and metalloids (Zhao et al. 2021). However, as indicated by the results of the present study, non-point source pollution of As is the main problem in the study area. Especially, the natural factors are probably more important than human activities. Therefore, the following aspects should be particularly considered for the treatment of As pollution in the study area.

- (1) High As groundwater can be very toxic to human health, and water should be treated before supplied to reduce the As concentration. Household arsenic

removal devices should be encouraged to residents living in the area. The method of adsorption and ion exchange is more suitable to be used as household filter material to remove arsenic from drinking water. The nanocomposites formed by some magnetic iron compounds such as magnetite–maghemite or jacobite with graphene (Abejón and Garea, 2015) or sand (Kango and Kumar, 2016) can be used as adsorption materials to remove arsenic ions from drinking water, which has less secondary pollution. In addition, cerium, as an adsorbent material in the latest research, combined with activated carbon (Li et al. 2021) or glass fiber (Sawana 2016), can also be used as a material for adsorption in household arsenic removal.

- (2) Because of the close relationship between phreatic groundwater and surface water, surface water quality should be strictly protected. Irrigation with water diverted from the Yellow River should be carefully allocated, as agricultural irrigation is an important factor affecting the release of As into groundwater. In addition, the As release mechanisms under irrigation infiltration should be further explored.
- (3) The infiltration of agricultural irrigation water in the study area is strong, so the use of As-containing pesticides and fertilizers should be regulated and the content of As in agricultural infiltration water should be tested regularly. If high As concentration is detected in irrigation water, it should be controlled.

## Conclusions

In this study, the hydrochemical characteristics which are important for the enrichment and variation of As in the phreatic groundwater in parts of the Yinchuan Plain have been discussed. Correlation analysis was used to quantify the degree of correlation among As and other ions. The Kriging interpolation method was used to draw the distribution maps of As and the ions. The impacts of As on human health were discussed. The main conclusions are as follows:

- (1) The ion abundance in the groundwater of the study area is  $\text{Na}^+ > \text{Mg}^{2+} > \text{Ca}^{2+} > \text{K}^+$  for cations, and  $\text{HCO}_3^- > \text{Cl}^- > \text{SO}_4^{2-}$  for anions. The dominant hydrochemical type of groundwater is  $\text{SO}_4\text{-Cl-Ca-Mg}$ , followed with  $\text{HCO}_3\text{-Ca-Mg}$  type, which are regulated by cation exchange, dissolution of carbonate, sulfate, and halite. There are a large number of water samples with exceeding  $\text{SO}_4^{2-}$ , Mn, and Fe.
- (2) The correlation analysis shows As has a positive correlation with  $\text{NH}_4\text{-N}$ ,  $\text{PO}_4^{3-}$ , Mn, and  $\text{HCO}_3^-$  in the dry season, while As has a negative correlation with As and  $\text{HCO}_3^-$ , Fe, and Mn in the wet season. The dis-

solution of manganese oxides containing As is the main source of As in phreatic water during the dry season. The infiltration of irrigation water affects the enrichment of As in the phreatic aquifer during the wet season.

- (3) In the dry season, high As is enriched in areas close to surface water, while in the wet season, the high As area extended to the western agricultural irrigation area, which is due to the irrigation that modifies the subsurface hydrogeochemical environment and leads to the temporal and spatial difference of As.
- (4) The health risk of lung cancer caused by As in groundwater is high in the study area as indicated by the linear fitting results. The lung cancer risk is higher than the maximum acceptable level. In order to solve this problem, it is necessary to make treatment before the water is supplied and irrigation with water diverted from the Yellow River should be carefully allocated. Irrigation water should be tested regularly for As concentration. Scientific research on As release mechanisms under the irrigation condition should be encouraged. Nanocomposites consisting of graphite and iron oxides or cerium complex can be used as adsorption material to remove arsenic from drinking water in domestic filtration system to reduce the health risk.

**Acknowledgements** We are grateful for the financial support received from the National Natural Science Foundation of China (42072286 and 41761144059), the Fundamental Research Funds for the Central Universities of CHD (300102299301), the Fok Ying Tong Education Foundation (161098), the China Postdoctoral Science Foundation (2016M590911 and 2017TT100719), the Shaanxi Postdoctoral Science Foundation (2016BSHTDZZ03), and the Ten Thousand Talents Program (W03070125).

## Declarations

**Conflict of interests** The authors declare that they have no conflicts of interest.

## References

- Abdalla O, RbY A-A (2013) Factors affecting groundwater chemistry in regional arid basins of variable lithology: example of Wadi Umairy, Oman. *Arab J Geosci* 7(7):2861–2870. <https://doi.org/10.1007/s12517-013-0981-7>
- Abejón R, Garea A (2015) A bibliometric analysis of research on arsenic in drinking water during the 1992–2012 period: An outlook to treatment alternatives for arsenic removal. *J Water Proc Eng* 6:105–119. <https://doi.org/10.1016/j.jwpe.2015.03.009>
- Ahmed MA, Abdel Samie SG, Badawy HA (2012) Factors controlling mechanisms of groundwater salinization and hydrogeochemical processes in the Quaternary aquifer of the Eastern Nile Delta, Egypt. *Environ Earth Sci* 68(2):369–394. <https://doi.org/10.1007/s12665-012-1744-6>

- Ahn JS (2012) Geochemical occurrences of arsenic and fluoride in bedrock groundwater: a case study in Geumsan County, Korea. *Environ Geochem Health* 34(Suppl 1):43–54. <https://doi.org/10.1007/s10653-011-9411-5>
- Ahn J, Boroje IJ, Ferdosi H, Kramer ZJ, Lamm SH (2020) Prostate cancer incidence in US counties and low levels of arsenic in drinking water. *Int J Environ Res Public Health* 17(3):960. <https://doi.org/10.3390/ijerph17030960>
- Alam MO, Shaikh WA, Chakraborty S, Avishek K, Bhattacharya T (2016) Groundwater arsenic contamination and potential health risk assessment of gangetic plains of Jharkhand, India. *Expo Health* 8:125–142. <https://doi.org/10.1007/s12403-015-0188-0>
- Islam ARMT, Shen SH, Bodrud-Doza M (2017) Assessment of arsenic health risk and source apportionment of groundwater pollutants using multivariate statistical techniques in Chapai-Nawabganj District, Bangladesh. *J Geol Soc India* 90(2):239–248. <https://doi.org/10.1007/s12594-017-0705-9>
- Arora R (2021) Nano adsorbents for removing the arsenic from waste/ground water for energy and environment management - a review. *Mater Today Proceed*. <https://doi.org/10.1016/j.matpr.2020.12.546>
- Baig JA, Kazi TG, Shah AQ, Afridi HI, Khan S, Kolachi NF, Kandhro GA, Wadhwa SK, Shah F (2011) Evaluation of toxic risk assessment of arsenic in male subjects through drinking water in southern Sindh Pakistan. *Biol Trace Elem Res* 143(2):772–786. <https://doi.org/10.1007/s12011-010-8933-5>
- Bargaoui ZK, Chebbi A (2009) Comparison of two kriging interpolation methods applied to spatiotemporal rainfall. *J Hydrol* 365(1):56–73. <https://doi.org/10.1016/j.jhydrol.2008.11.025>
- Basu A, Mahata J, Gupta S, Giri AK (2001) Genetic toxicology of a paradoxical human carcinogen, arsenic: a review. *Mutation Research/Fundamental and Molecular Mechanisms of Mutagenesis* 488(2):171–194. [https://doi.org/10.1016/S1383-5742\(01\)0056-4](https://doi.org/10.1016/S1383-5742(01)0056-4)
- Basu A, Saha D, Saha R, Ghosh T, Saha B (2013) A review on sources, toxicity and remediation technologies for removing arsenic from drinking water. *Res Chem Intermed* 40(2):447–485. <https://doi.org/10.1007/s11164-012-1000-4>
- Bian J, Wang Y, Zhao J (2015) Arsenic and fluorine in groundwater in western Jilin Province, China: occurrence and health risk assessment. *Nat Hazards* 77(3):1903–1914. <https://doi.org/10.1007/s11069-015-1682-1>
- Bibi M, Hashmi MZ, Malik RN (2015) Human exposure to arsenic in groundwater from Lahore district, Pakistan. *Environ Toxicol Pharmacol* 39(1):42–52. <https://doi.org/10.1016/j.etap.2014.10.020>
- Biswas A, Biswas B, Santra SC (2013) Arsenic in irrigated water, soil, and rice: perspective of the cropping seasons. *Paddy and Water Environmental* 12(4):407–412. <https://doi.org/10.1007/s10333-013-0396-9>
- Bräuner EV, Nordsborg RB, Andersen ZJ, Tjønneland A, Loft S, Raaschou-Nielsen O (2014) Long-term exposure to low-level arsenic in drinking water and diabetes incidence: a prospective study of the diet, cancer and health cohort. *Environ Health Perspect* 122(10):1059–1065. <https://doi.org/10.1289/ehp.1408198>
- Brunner PH, Baccini P (1992) Regional material management and environmental protection. *Waste Manag Res* 10(2):203–212. [https://doi.org/10.1016/0734-242X\(92\)90073-T](https://doi.org/10.1016/0734-242X(92)90073-T)
- Chakraborty D, Rahman MM, Ahamed S, Dutta RN, Pati S, Mukherjee SC (2016) Arsenic groundwater contamination and its health effects in Patna district (capital of Bihar) in the middle Ganga plain, India. *Chemosphere* 152:520–529. <https://doi.org/10.1016/j.chemosphere.2016.02.119>
- Chen J, Qian H, Wu H, Gao Y, Li X (2017) Assessment of arsenic and fluoride pollution in groundwater in Dawukou area, Northwest China, and the associated health risk for inhabitants. *Environ Earth Sci* 76(8):314. <https://doi.org/10.1007/s12665-017-6629-2>

- Cotruvo J, Bartram J (2009) Calcium and magnesium in drinking-water: public health significance. World Health Organization, Geneva
- Delgado C, Pacheco J, Cabrera A, Batllori E, Orellana R, Bautista F (2010) Quality of groundwater for irrigation in tropical karst environment: the case of Yucatán, Mexico. *Agric Water Manag* 97(10):1423–1433. <https://doi.org/10.1016/j.agwat.2010.04.006>
- Duan Y (2016) Seasonal variations of groundwater arsenic concentration in shallow aquifers at Jiangnan plain. PhD Thesis, China University of Geosciences, Wuhan (in Chinese)
- Guagliardi I, Cicchella D, De Rosa R (2012) A geostatistical approach to assess concentration and spatial distribution of heavy metals in urban soils. *Water Air Soil Pollut* 223:5983–5998. <https://doi.org/10.1007/s11270-012-1333-z>
- General Administration of Quality Supervision, Inspection & Quarantine of China and Standardization Administration of China (2017) Standard for groundwater quality (GB/T 14848–2017). Available at <http://www.shanghai.gov.cn/bm/hbj/zwgk/hjjc/202007/P020200727326446952905.pdf>, accessed 24th, 2021 (in Chinese)
- Guo H, Wen D, Liu Z, Jia Y, Guo Q (2014) A review of high arsenic groundwater in Mainland and Taiwan, China: Distribution, characteristics and geochemical processes. *Appl Geochem* 41:196–217. <https://doi.org/10.1016/j.apgeochem.2013.12.016>
- He S, Li P (2020a) A MATLAB based graphical user interface (GUI) for quickly producing widely used hydrogeochemical diagrams. *Geochemistry* 80(4):125550. <https://doi.org/10.1016/j.chemer.2019.125550>
- He X, Li P (2020b) Surface water pollution in the middle Chinese Loess Plateau with special focus on hexavalent chromium (Cr<sup>6+</sup>): occurrence, sources and health risks. *Expo Health* 12(3):385–401. <https://doi.org/10.1007/s12403-020-00344-x>
- He X, Li P, Ji Y, Wang Y, Su Z, Elumalai V (2020a) Groundwater arsenic and fluoride and associated arsenicosis and fluorosis in China: occurrence, distribution and management. *Expo Health* 12(3):355–368. <https://doi.org/10.1007/s12403-020-00347-8>
- He X, Li P, Wu J, Wei M, Ren X, Wang D (2020b) Poor groundwater quality and high potential health risks in the Datong Basin, northern China: research from published data. *Environ Geochem Health*. <https://doi.org/10.1007/s10653-020-00520-7>
- Hu H, Shu H (2015) An improved coarse-grain parallel algorithm for computational acceleration of ordinary Kriging interpolation. *Comput Geosci*. <https://doi.org/10.1016/j.cageo.2015.02.011>
- Jang C, Lin K, Liu C, Lin M (2008) Risk-based assessment of arsenic-affected aquacultural water in blackfoot disease hyperendemic areas. *Stochastic Environ Res Risk Assess* 23(5):603–612. <https://doi.org/10.1007/s00477-008-0245-3>
- Ji Y, Wu J, Wang Y, Elumalai V, Subramani T (2020) Seasonal variation of drinking water quality and human health risk assessment in Hancheng City of Guanzhong Plain, China. *Expo Health* 12(3):469–485. <https://doi.org/10.1007/s12403-020-00357-6>
- Kango S, Kumar R (2016) Magnetite nanoparticles coated sand for arsenic removal from drinking water. *Environmental Earth Sciences*. <https://doi.org/10.1007/s12665-016-5282-5>
- Khan KM, Chakraborty R, Bundschuh J, Bhattacharya P, Parvez F (2020) Health effects of arsenic exposure in Latin America: An overview of the past eight years of research. *Sci Total Environ* 710:136071. <https://doi.org/10.1016/j.scitotenv.2019.136071>
- Lamm S, Boroje I, Ferdosi H, Ahn J (2018) Lung Cancer Risk and Low ( $\leq 50$   $\mu\text{g/L}$ ) Drinking Water Arsenic Levels for US Counties (2009–2013)—A Negative Association. *Int J Environ Res Public Health* 15(6):1200. <https://doi.org/10.3390/ijerph15061200>
- Li P (2014) Research on groundwater environment under human interferences: a case study from Weining plain, Northwest China. PhD Thesis, Chang'an University, Xi'an (in Chinese)
- Li P (2016) Groundwater quality in western china: challenges and paths forward for groundwater quality research in western China. *Expo Health* 8(3):305–310. <https://doi.org/10.1007/s12403-016-0210-1>
- Li P, Wu J, Qian H (2012) Assessment of groundwater quality for irrigation purposes and identification of hydrogeochemical evolution mechanisms in Pengyang County, China. *Environ Earth Sci* 69(7):2211–2225. <https://doi.org/10.1007/s12665-012-2049-5>
- Li P, Qian H, Wu J, Zhang Y, Zhang H (2013) Major ion chemistry of shallow groundwater in the Dongsheng Coalfield, Ordos Basin, China. *Mine Water Environ* 32(3):195–206. <https://doi.org/10.1007/s10230-013-0234-8>
- Li P, Qian H, Howard KWF, Wu J, Lyu X (2014) Anthropogenic pollution and variability of manganese in alluvial sediments of the Yellow River, Ningxia, northwest China. *Environ Monit Assess* 186(3):1385–1398. <https://doi.org/10.1007/s10661-013-3461-3>
- Li P, Qian H, Wu J (2015) Hydrochemical appraisal of groundwater quality for drinking and irrigation purposes and the major influencing factors: a case study in and around Hua County, China. *Arab J Geosci* 9(1):15. <https://doi.org/10.1007/s12517-015-2059-1>
- Li P, Wu J, Qian H, Zhang Y, Yang N, Jing L, Yu P (2016) Hydrogeochemical characterization of groundwater in and around a wastewater irrigated forest in the southeastern edge of the Tengger Desert, northwest China. *Expo Health* 8(3):331–348. <https://doi.org/10.1007/s12403-016-0193-y>
- Li P, Tian R, Xue C, Wu J (2017) Progress, opportunities and key fields for groundwater quality research under the impacts of human activities in China with a special focus on western China. *Environ Sci Pollut Res* 24(15):13224–13234. <https://doi.org/10.1007/s11356-017-8753-7>
- Li R, Kuo Y, Liu W, Jang C, Zhao E, Yao L (2018) Potential health risk assessment through ingestion and dermal contact arsenic-contaminated groundwater in Jiangnan Plain, China. *Environ Geochem Health* 40(4):1585–1599. <https://doi.org/10.1007/s10653-018-0073-4>
- Li R, Yang W, Gao S, Shang J, Li Q (2021) Hydrous cerium oxides coated glass fiber for efficient and long-lasting arsenic removal from drinking water. *J Adv Ceram* 10(2):247–257. <https://doi.org/10.1007/s40145-020-0435-0>
- Lidia RJ (2014) Calcium and magnesium in groundwater: occurrence and significance for human health. Taylor & Francis Group, London
- Maity J, Ho P, Huang Y, Sun A, Chen C, Chen C (2019) The removal of arsenic from arsenic-bearing groundwater in In-situ and Ex-situ environment using novel natural magnetic rock material and synthesized magnetic material as adsorbent: a comparative assessment. *Environ Pollut* 253:768–778. <https://doi.org/10.1016/j.envpol.2019.07.048>
- McBean EA (2012) Risk characterization for arsenic-impacted water sources, including ground-truthing. *Stoch Env Res Risk Assess* 27(3):705–711. <https://doi.org/10.1007/s00477-012-0633-6>
- Ministry of Health of the PRC, Standardization Administration of the PRC (2006) Standards for drinking water quality (GB5749–2006). China Standard Press, Beijing (in Chinese)
- Qian H, Li P, Howard KWF, Yang C, Zhang X (2012) Assessment of groundwater vulnerability in the Yinchuan Plain, northwest China Using OREADIC. *Environ Monit Assess* 184(6):3613–3628. <https://doi.org/10.1007/s10661-011-2211-7>
- Qian H, Li P, Wu J, Zhou Y (2013) Isotopic Characteristics of precipitation, surface and ground waters in the Yinchuan Plain, northwest China. *Environ Earth Sci* 70(1):57–70. <https://doi.org/10.1007/s12665-012-2103-3>
- Qian H, Wu J, Zhou Y, Li P (2014) Stable oxygen and hydrogen isotopes as indicators of lake water recharge and evaporation in the lakes of the Yinchuan Plain. *Hydrol Process* 28:3554–3562. <https://doi.org/10.1002/hyp.9915>

- Radford M, Yunesian M, Nabizadeh R, Biglari H, Nazmara S, Hadi M, Yousefi N, Yousefi M, Abbasnia A, Mahvi AH (2018) Drinking water quality and arsenic health risk assessment in Sistan and Baluchestan, Southeastern province, Iran. *Hum Ecol Risk Assess Int J* 25(4):949–965. <https://doi.org/10.1080/10807039.2018.1458210>
- Ren X, Li P, He X, Su F, Elumalai V (2021) Hydrogeochemical processes affecting groundwater chemistry in the central part of the Guanzhong Basin, China. *Arch Environ Contam Toxicol* 80(1):74–91. <https://doi.org/10.1007/s00244-020-00772-5>
- Rice EW, Baird RB, Eaton AD (2017) Standard methods for the examination of water and wastewater, 23rd edn. American Public Health Association, Washington
- Roman-Ross G, Cuello G, Turrillas X, Fernandez-Martinez A, Charlet L (2006) Arsenite sorption and co-precipitation with calcite. *Chem Geol* 233(3–4):328–336. <https://doi.org/10.1016/j.chemgeo.2006.04.007>
- Sawana R, Somasundar Y, Iyer VS, Baruwati B (2016) Ceria modified activated carbon: an efficient arsenic removal adsorbent for drinking water purification. *Appl Water Sci* 7(3):1223–1230. <https://doi.org/10.1007/s13201-016-0398-z>
- Smedley PL, Kinniburgh DG, Macdonald DMJ, Nicolli HB, Barros AJ, Tullio JO, Pearce JM, Alonso MS (2005) Arsenic associations in sediments from the loess aquifer of La Pampa, Argentina. *Appl Geochem* 20(5):989–1016. <https://doi.org/10.1016/j.apgeochem.2004.10.005>
- Su Z, Wu J, He X, Elumalai V (2020) Temporal changes of groundwater quality within the groundwater depression cone and prediction of confined groundwater salinity using Grey Markov model in Yinchuan area of northwest China. *Expo Health* 12(3):447–468. <https://doi.org/10.1007/s12403-020-00355-8>
- Sultana J, Farooqi A, Ali U (2014) Arsenic concentration variability, health risk assessment, and source identification using multivariate analysis in selected villages of public water system, Lahore, Pakistan. *Environ Monit Assess* 186(2):1241–1251. <https://doi.org/10.1007/s10661-013-3453-3>
- Tian M, Ma X, Jia J, Qiao Y, Wu T, Li H, Liu Y (2017) Study of residents' exposure to arsenic near the Yellow River Gan-Ning-Meng reaches using inductively coupled plasma mass spectrometry. *Spectroscopy and Spectral Analysis* 37(5):1628–1633. [https://doi.org/10.3964/j.issn.1000-0593\(2017\)05-1628-06](https://doi.org/10.3964/j.issn.1000-0593(2017)05-1628-06)
- Wang S, Li W, Chen C, Huang Y, Chen J, Chang K, Chou K (2011) Hypertension incidence after tap-water implementation: A 13-year follow-up study in the arseniasis-endemic area of south-western Taiwan. *Sci Total Environ* 409(21):4528–4535. <https://doi.org/10.1016/j.scitotenv.2011.07.058>
- Wang D, Wu J, Wang Y, Ji Y (2020) Finding high-quality groundwater resources to reduce the hydatidosis incidence in the Shiqu County of Sichuan Province, China: analysis, assessment, and management. *Expo Health* 12(2):307–322. <https://doi.org/10.1007/s12403-019-00314-y>
- Welch K, Higgins I, Oh M, Burchfiel C (1982) Arsenic exposure, smoking, and respiratory cancer in copper smelter workers. *Arch Environ Health* 37(6):325–335. <https://doi.org/10.1080/00039896.1982.10667586>
- Wen D, Zhang F, Zhang E, Wang C, Han S, Zheng Y (2013) Arsenic, fluoride and iodine in groundwater of China. *J Geochem Explor* 135:1–21. <https://doi.org/10.1016/j.gexplo.2013.10.012>
- WHO (2011) Guidelines for drinking water quality, 4th edn. World Health Organization, Geneva, 978–92–4–154815–1
- Wu J, Li P, Qian H, Chen J (2013) Groundwater pollution in and around a paper wastewater-irrigated area, northwest China. In: 2013 fourth international conference on digital manufacturing and automation (ICDMA 2013), Qingdao, China, 2013. IEEE Press, New York, pp 649–652. <https://doi.org/https://doi.org/10.1109/ICDMA.2013.154>
- Wu J, Li P, Qian H, Duan Z, Zhang X (2014) Using correlation and multivariate statistical analysis to identify hydrogeochemical processes affecting the major ion chemistry of waters: Case study in Laoheba phosphorite mine in Sichuan, China. *Arab J Geosci* 7(10):3973–3982. <https://doi.org/10.1007/s12517-013-1057-4>
- Wu J, Li P, Qian H (2015) Hydrochemical characterization of drinking groundwater with special reference to fluoride in an arid area of China and the control of aquifer leakage on its concentrations. *Environ Earth Sci* 73(12):8575–8588. <https://doi.org/10.1007/s12665-015-4018-2>
- Wu J, Wang L, Wang S, Tian R, Xue C, Feng W, Li Y (2017) Spatiotemporal variation of groundwater quality in an arid area experiencing long-term paper wastewater irrigation, northwest China. *Environ Earth Sci* 76(13):460. <https://doi.org/10.1007/s12665-017-6787-2>
- Wu J, Li P, Wang D, Ren X, Wei M (2020) Statistical and multivariate statistical techniques to trace the sources and affecting factors of groundwater pollution in a rapidly growing city on the Chinese Loess Plateau. *Hum Ecol Risk Assess* 26(6):1603–1621. <https://doi.org/10.1080/10807039.2019.1594156>
- Zhao J, Zhen G, Liu F, Sun Q, Li T, Wei J, Liu Y, Shu Z (2014) Dose-response relationship between arsenic exposure through drinking water and incidence of lung cancer a meta-analysis. *J Environ Health* 31(4):319–322. <https://doi.org/10.16241/j.cnki.1001-5914.2014.04.012> (in Chinese)
- Zhao H, Song F, Su F, Shen Y, Li P (2021) Removal of cadmium from contaminated groundwater using a novel silicon/aluminum nanomaterial: an experimental study. *Arch Environ Contam Toxicol* 80(1):234–247. <https://doi.org/10.1007/s00244-020-00784-1>

**Publisher's Note** Springer Nature remains neutral with regard to jurisdictional claims in published maps and institutional affiliations.